Improved Numerical Methods for the Simulation of Microwave Circuits

G. Hebermehl *
R. Schlundt †

Weierstrass Institute for Applied Analysis and Stochastics, Mohrenstr. 39, D-10117 Berlin, Germany

H. Zscheile ‡

W. Heinrich §

Ferdinand-Braun-Institut für Höchstfrequenztechnik, Rudower Chaussee 5, D-12489 Berlin, Germany

December 22, 1998

1991 Mathematics Subject Classification.
35Q60, 65F10, 65F15, 65N22.
Keywords.
Microwave device simulation, scattering matrix, Maxwellian equations, boundary value problem, finite-volume method, eigenvalue problem, system of linear algebraic equations.

*e-mail: hebermehl@wias-berlin.de, URL: http://hyperg.wias-berlin.de
†e-mail: schlundt@wias-berlin.de, URL: http://hyperg.wias-berlin.de
‡e-mail: zscheile@fbh.fta-berlin.de, URL: http://www.fta-berlin.de
§e-mail: heinrich@fbh.fta-berlin.de, URL: http://www.fta-berlin.de

Abstract

The scattering matrix describes monolithic microwave integrated circuits that are connected to transmission lines in terms of their wave modes. Using a finite-volume method the corresponding boundary value problem of Maxwell's equations can be solved by means of a two-step procedure. An eigenvalue problem for non-symmetric matrices yields the wave modes. The eigenfunctions determine the boundary values at the ports of the transmission lines for the calculation of the fields in the three dimensional structure. The electromagnetic fields and the matrix elements are achieved by the solution of large-scale systems of linear equations with indefinite symmetric matrices. Improved numerical solutions for the time and memory consuming problems are treated in this paper. Numerical results are discussed for real life problems. The numerical effort could be reduced considerably. This paper is a revised version of the preprint No. 378.

Contents

1 Introduction **2**

2 Scattering Matrix **4**

3 Boundary Value Problem **5**

4 Matrix Representation of the Maxwellian Equations **6**

5 System of Linear Algebraic Equations **7**

6 Eigenvalue Problem **11**

7 Numerical Results **13**

7.1 Numerical Example for the System of Linear Algebraic Equations 14

7.2 Numerical Examples for the Eigenvalue Problem 15

List of Figures

1 Example of discretized structure: coupled spiral inductors. x direction on a larger scale 3

List of Tables

1 Performance comparisions of different preconditioners compared to the original version for the calculation of the scattering matrix of the right-hand side of the structure consisting of coupled spiral inductors. 15
2 Comparisions of computing times for the eigenvalue problem between the original and the new version for a lossfree and a lossy example. 16

1 Introduction

The design of monolithic microwave integrated circuits (MMIC) requires efficient CAD tools in order to avoid costly and time-consuming redesign cycles.

The electromagnetic characteristics of microwave circuits and packages can be described by equivalent circuits in terms of voltages and currents or by the scattering matrix. With growing frequencies the voltage and current definitions become ambiguous and the scattering matrix approach is more appropriate. In order to determine the scattering matrix, the circuit is inserted between transmission lines. As an example, Figure 1 shows a structure consisting of two spiral inductors. The coupling between them had to be calculated. The current is fed by four coplanar transmission lines. Only short parts of them are shown in the figure. For typical microwave packages one is dealing with transmission lines of the microstrip or coplanar type. The scattering matrix describes the structure in terms of wave modes on these lines. In this way, a three dimensional boundary-value problem can be formulated using the Maxwellian equations in frequency domain in order to compute the electromagnetic field and, subsequently, the scattering matrix.

We solve the problem numerically by the so-called Finite Difference Method in Frequency Domain (FDFD) [1], [2], [3]. The field volume is subdivided into rectangular cells, and the Maxwellian partial differential equations are approximated by difference equations. They can be set up by the method of

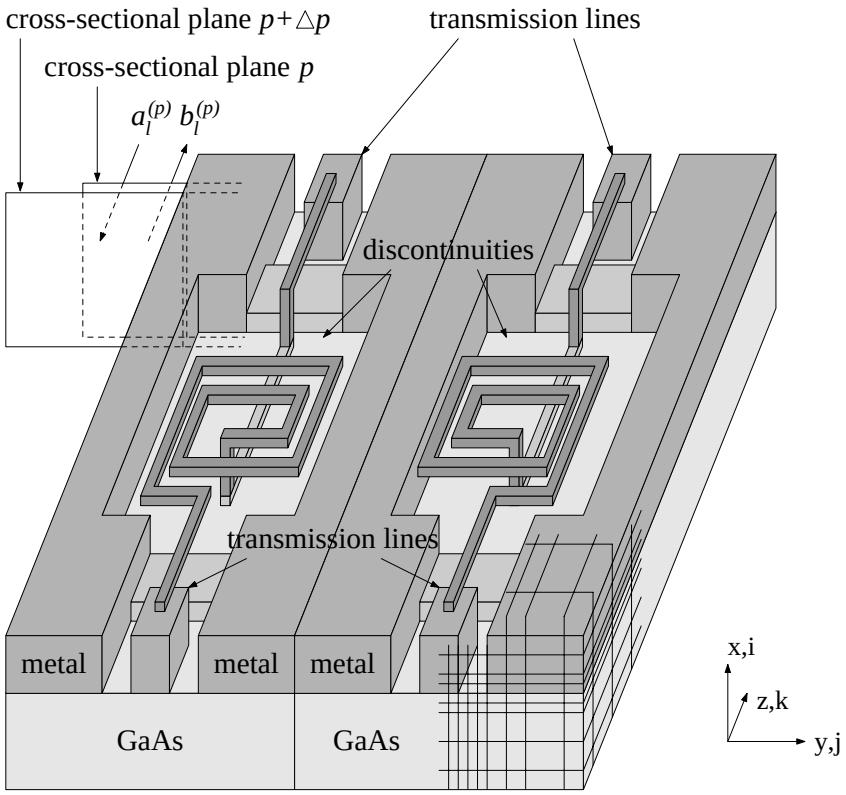

Figure 1: Example of discretized structure: coupled spiral inductors. x direction on a larger scale

finite integration, using the integral formulation of Maxwell's equations for each cell.

Working in the frequency domain is superior to the more common time domain approach in certain cases: The scattering matrix of a given structure can be calculated for an arbitrary number of simultaneously excited modes. For structures with electrically small geometric details the frequency domain allows shorter computing times, because with the time domain small cell sizes require an excessive number of small time steps for stability reasons. The time domain approach does not provide mode separation in contrast to FDFD.

2 Scattering Matrix

The structure under investigation consists of infinitely long transmission lines and a discontinuity (see Figure 1). The transmission lines are assumed to be longitudinally homogeneous. The discontinuity may have an arbitrary structure. The fields are computed in a rectangular volume, which contains the discontinuity and short parts of the transmission lines. Ports are defined on the transmission lines. The remaining surface of the computational volume is formed by electric or magnetic walls. The incoming modes a_l are changed in the discontinuity. The changed outgoing modes are denoted with b_l. The scattering matrix S describes the energy exchange and phase relation between all outgoing modes $b_l^{(p)}$ and all incoming modes $a_l^{(p)}$ [4]:

$$b_{\rho,\nu} = \sum_{\sigma=1}^{m_s} S_{\rho,\sigma} a_{\sigma,\nu}, \quad S = \begin{pmatrix} S_{11} & S_{12} & \cdots & S_{1m_s} \\ S_{21} & S_{22} & \cdots & S_{2m_s} \\ \cdots & \cdots & \cdots & \cdots \\ S_{m_s1} & S_{m_s2} & \cdots & S_{m_sm_s} \end{pmatrix} = (S_{\rho,\sigma}), \qquad (1)$$

$$\nu, \rho, \sigma = 1(1)m_s, \quad m_s = \sum_{p=1}^{\overline{p}} m^{(p)}. \qquad (2)$$

$m^{(p)}$ is the number of modes which have to be taken into account on the port p. $\overline{p}$ is the number of ports. The modes on a port p are numbered with l. Then the indices ρ (and σ) are related to the mode l in the following way

$$\rho = l + \sum_{q=1}^{p-1} m^{(q)}. \qquad (3)$$

The scattering matrix can be extracted from the orthogonal decomposition of the electric field at a pair of two neighboring cross-sectional planes p and $p + \Delta p$ (see Figure 1) on each waveguide for a number of linear independent excitations of the transmission lines [4].

3 Boundary Value Problem

We use the integral form of the Maxwellian equations in the frequency domain:

$$\begin{aligned} \oint_{\partial\Omega} \frac{1}{\tilde{\mu}\mu_0}\vec{B}\cdot d\vec{s} &= \int_{\Omega}(\jmath\omega\tilde{\epsilon}\epsilon_0\vec{E})\cdot d\vec{\Omega}, \quad \oint_{\cup\Omega}(\tilde{\epsilon}\epsilon_0\vec{E})\cdot d\vec{\Omega} = 0, \\ \oint_{\partial\Omega}\vec{E}\cdot d\vec{s} &= \int_{\Omega}(-\jmath\omega\vec{B})\cdot d\vec{\Omega}, \quad \oint_{\cup\Omega}\vec{B}\cdot d\vec{\Omega} = 0 \end{aligned} \tag{4}$$

taking into account the constitutive relations

$$\vec{B} = \mu\vec{H}, \;\; \vec{D} = \epsilon\vec{E}, \;\; \text{with } \underline{\epsilon} = \epsilon + \frac{\kappa}{\jmath\omega}, \;\; \mu = \tilde{\mu}\mu_0, \;\; \underline{\epsilon} = \tilde{\epsilon}\epsilon_0. \tag{5}$$

The electric and the magnetic field intensity $\vec{E}$ and $\vec{H}$, and the electric and magnetic flux density $\vec{D}$ and $\vec{B}$, respectively, are complex functions of the spatial coordinates only. ω is the angular frequency and $\jmath^2 = -1$. The permeability μ, the permittivity ϵ, and the conductivity κ are assumed to be scalar functions of the spatial coordinates.

At the port p the transverse electric field $\vec{E}_t(z_p)$ is given by superposing all transmission line modes $\vec{E}_{t,l}(z_p)$ with weighted mode-amplitude sums $w_l(z_p)$:

$$\vec{E}_t(z_p) = \sum_{l=1}^{m^{(p)}} w_l(z_p)\vec{E}_{t,l}(z_p). \tag{6}$$

The transverse electric mode fields $\vec{E}_{t,l}^{(p)} = \vec{E}_{t,l}(z_p)$ are computed using an eigenvalue problem for transmission lines (see section 6).

At all other parts of the enclosure the tangential electric or magnetic field is assumed to be zero:

$$\vec{E}_{tang} = 0 \quad \text{or} \quad \vec{H}_{tang} = 0. \tag{7}$$

The transverse mode fields $\vec{E}_{t,l}(z_p)$ satisfy an orthogonality relation

$$\int_{\Omega}(\vec{E}_{t,l}(z_p)\times\vec{H}_{t,m})\cdot d\vec{\Omega} = \eta_m\delta_{l,m}. \tag{8}$$

The mode amplitudes of the transverse electric fields are normalized:

$$\mid \eta_m \mid = 1\text{Watt}. \tag{9}$$

The orthogonality relation (8) is applied at two neighboring cross-sectional planes z_p and $z_p + \Delta z_p$:

$$\begin{aligned} \tfrac{1}{\eta_m} \int\limits_{\Omega} (\vec{E}_t^{(p)} \times \vec{H}_{t,m}^{(p)}) \cdot d\vec{\Omega} &= a_m^{(p)} + b_m^{(p)} &&= w_m^{(p)}, \\ \tfrac{1}{\eta_m} \int\limits_{\Omega} (\vec{E}_t^{(p+\Delta p)} \times \vec{H}_{t,m}^{(p)}) \cdot d\vec{\Omega} &= a_m^{(p+\Delta p)} + b_m^{(p+\Delta p)} &&= w_m^{(p+\Delta p)}. \end{aligned} \tag{10}$$

The weighted mode-amplitude sums $w_l^{(p)}$ are given. Because of

$$a_m^{(p+\Delta p)} = a_m^{(p)} e^{-\jmath k_{z_l}^{(p)} \Delta z_p}, \qquad b_m^{(p+\Delta p)} = b_m^{(p)} e^{+\jmath k_{z_l}^{(p)} \Delta z_p} \tag{11}$$

we can compute the mode amplitudes $a_m^{(p)}$ and $b_m^{(p)}$ from (10), and subsequently, the scattering matrix (1). $k_{z_l}^{(p)}, l = 1(1)m^{(p)}$, are the propagation constants (see section 6) at the port p.

4 Matrix Representation of the Maxwellian Equations

The region is divided into elementary cells (see Figure 1) using a three dimensional nonequidistant orthonormal Cartesian grid. We use staggered grids [5], [6]. The electric field components are located at the centers of the edges of the cell and the magnetic flux density components are normal to the centers of the faces. Thus, the electric field components form a primary grid, and the magnetic flux density components a dual grid. We use the lowest-order integration formulae

$$\oint_{\partial\Omega} \vec{f} \cdot d\vec{s} \approx \sum (\pm f_i s_i), \quad \int_{\Omega} \vec{f} \cdot d\vec{\Omega} \approx f\Omega \tag{12}$$

in order to approximate Maxwellian equations (4). Thus, we get the matrix representation of (4):

$$\begin{aligned} A^T D_{s/\tilde{\mu}} \vec{b} &= \jmath\omega\epsilon_0\mu_0 D_{A_{\tilde{\epsilon}}} \vec{e}, & B D_{A_{\tilde{\epsilon}}} \vec{e} &= 0, \\ A D_s \vec{e} &= -\jmath\omega D_A \vec{b}, & B^T D_A \vec{b} &= 0. \end{aligned} \tag{13}$$

The vectors $\vec{e}$ and $\vec{b}$ contain the components of the electric field intensity and the components of the magnetic flux density of the elementary cells, respectively. The diagonal matrices $D_{s/\tilde{\mu}}$, $D_{A_{\tilde{\epsilon}}}$, D_s, and D_A contain the information on cell dimension and material for the specified structure and the corresponding mesh. A is defined as the operator of the line integral in the second Maxwellian equation (left formula of the second row of (4)) using the primary grid. B represents the surface integral of the divergence. A and B are sparse, and contain the values 1, -1 and 0 only.

5 System of Linear Algebraic Equations

Eliminating the components of the magnetic flux density from the two equations of the left-hand side of (13) we get the system of linear algebraic equations

$$Q_1\vec{e} = 0, \quad Q_1 = A^T D_{s/\tilde{\mu}} D_A^{-1} A D_s - k_0^2 D_{A_{\tilde{\epsilon}}}, \quad k_0 = \omega\sqrt{\epsilon_0\mu_0}. \tag{14}$$

The ingoing wave modes at the ports of the structure act as sources for the field inside the discontinuity. Thus, a source term has to be induced by partitioning of the matrix Q_1:

$$Q_1 = Q_{1,A} + Q_{1,r}, \quad Q_{1,A}\vec{e} = -Q_{1,r}\vec{e}, \tag{15}$$

where $Q_{1,r}\vec{e}$ is known. Using $\vec{r} = -Q_{1,r}\vec{e}$ the matrix $Q_{1,A}$ is transformed into the symmetric matrix $\tilde{Q}_{1,A}$, after some manipulations:

$$\tilde{Q}_{1,A}\tilde{\vec{e}} = D_s^{\frac{1}{2}} Q_{1,A} D_s^{-\frac{1}{2}} D_s^{\frac{1}{2}}\vec{e} = -D_s^{\frac{1}{2}} Q_{1,r}\vec{e} = D_s^{\frac{1}{2}}\vec{r} = \tilde{\vec{r}}. \tag{16}$$

Now, we take advantage of the fact that there is no space charge in our volume, and therefore $\mathrm{div}(\tilde{\epsilon}\epsilon_0\vec{E}) = 0$. The gradient of the electric-field divergence

$$\tilde{\epsilon}\epsilon_0 \nabla\left(\frac{1}{(\tilde{\epsilon}\epsilon_0)^2}\nabla\cdot\tilde{\epsilon}\epsilon_0\vec{E}\right) = 0 \tag{17}$$

is equivalent to the matrix equation

$$Q_2\vec{e} = 0 \quad \text{with} \quad Q_2 = D_s^{-1} D_{A_{\tilde{\epsilon}}} B^T D_{V_{\tilde{\epsilon}\tilde{\epsilon}}}^{-1} B D_{A_{\tilde{\epsilon}}}. \tag{18}$$

The elements of the diagonal matrix $D_{V_{\tilde{\epsilon}\tilde{\epsilon}}}$ contain the information on cell dimension and material $\tilde{\epsilon}\epsilon_0$ for the 8 partial volumes of the dual elementary cells used for the computation of (17) [4], [7].
We carry out a similar partitioning like (15) for Equation (18):

$$Q_2 = Q_{2,A} + Q_{2,r}. \tag{19}$$

Using $Q_{2,r}\vec{e} = 0$ the matrix $Q_{2,A}$ is transformed into the symmetric matrix $\tilde{Q}_{2,A}$, after some manipulations:

$$\tilde{Q}_{2,A}\vec{\tilde{e}} = D_s^{\frac{1}{2}} Q_{2,A} D_s^{-\frac{1}{2}} D_s^{\frac{1}{2}} \vec{e} = -D_s^{\frac{1}{2}} Q_{2,r}\vec{e} = 0, \quad \vec{\tilde{e}} = D_s^{\frac{1}{2}}\vec{e}. \tag{20}$$

Adding Equation (20) to (16) the new system can be solved numerically faster [1].
The high-dimensional indefinite symmetric system of linear algebraic equations (see (14), (16), (20)) with multiple right hand sides

$$U\vec{\tilde{e}} = \vec{\tilde{r}}, \quad U = \quad D_s^{\frac{1}{2}} Q_{1,A} D_s^{-\frac{1}{2}} = \tilde{Q}_{1,A}, \tag{21}$$

$$V\vec{\tilde{e}} = 0, \quad V = \quad D_s^{\frac{1}{2}} Q_{2,A} D_s^{-\frac{1}{2}} = \tilde{Q}_{2,A} \tag{22}$$

is solved using iterative methods. The number of right hand sides is m_s (see (2)).

The convergence rate of iterative methods depends on spectral properties of the coefficient matrix U. Thus, we transform the linear system (21) into one that is equivalent in the sense that is has the same solution but more favorable spectral properties. A preconditioner $M = M_1 M_2$ is a matrix that performs such a transformation:

$$M_1^{-1} U M_2^{-1} (M_2 \vec{\tilde{e}}) = M_1^{-1} \vec{\tilde{r}} \tag{23}$$

We use four kinds of preconditioning:

1. The effect of the addition of the two equations (16) and (20) described above can be interpreted as preconditioning. Using (22) we construct a preconditioner M for the original system (21):

   $$M_1^{-1} = I + VU^{-1}, \quad M_1 = (I + VU^{-1})^{-1}, \quad M_2 = I. \tag{24}$$

   Substituting (24) in (23) we get

   $$(I + VU^{-1})U\vec{\tilde{e}} = (I + VU^{-1})\vec{\tilde{r}} \Rightarrow (U + V)\vec{\tilde{e}} = \vec{\tilde{r}} + V\vec{\tilde{e}} = \vec{\tilde{r}} \tag{25}$$

or

$$\tilde{U}\vec{\tilde{e}} = \vec{\tilde{r}} \quad \text{with} \quad \tilde{U} = U + V. \tag{26}$$

2. A commonly used approach for solving large sparse linear systems is to find sets of unknowns which are independent. A set of such unknowns is called an independent set. Independent set orderings are permutations $\tilde{P}$ to transform the system (26) into the form

$$\tilde{P}\tilde{U}\tilde{P}^T\vec{t} = \begin{pmatrix} \tilde{D} & \tilde{E}^T \\ \tilde{E} & \tilde{H} \end{pmatrix} \begin{pmatrix} \vec{t}_1 \\ \vec{t}_2 \end{pmatrix} = \begin{pmatrix} \vec{s}_1 \\ \vec{s}_2 \end{pmatrix} \tag{27}$$

with

$$\vec{t} = \tilde{P}\vec{\tilde{e}} = \begin{pmatrix} \vec{t}_1 \\ \vec{t}_2 \end{pmatrix}, \qquad \vec{s} = \tilde{P}\vec{\tilde{r}} = \begin{pmatrix} \vec{s}_1 \\ \vec{s}_2 \end{pmatrix}. \tag{28}$$

$\tilde{D}$ is a diagonal matrix, $\tilde{E}$ is a general sparse matrix, and $\tilde{H}$ is a quadratic sparse matrix. The unknowns of the independent set $\tilde{D}$ are eliminated to get the next reduced matrix

$$\hat{U} = \tilde{H} - \tilde{E}\tilde{D}^{-1}\tilde{E}^T, \tag{29}$$

and we have to solve the system of linear equations

$$\hat{U}\vec{t}_2 = (\tilde{H} - \tilde{E}\tilde{D}^{-1}\tilde{E}^T)\vec{t}_2 = \vec{s}_2 - \tilde{E}\tilde{D}^{-1}\vec{s}_1 \tag{30}$$

or

$$\hat{U}\vec{\hat{e}} = \vec{\hat{r}}, \quad \hat{U} = \tilde{H} - \tilde{E}\tilde{D}^{-1}\tilde{E}^T, \ \vec{\hat{e}} = \vec{t}_2, \ \vec{\hat{r}} = \vec{s}_2 - \tilde{E}\tilde{D}^{-1}\vec{s}_1. \tag{31}$$

Thus, we get

$$\vec{t}_1 = \tilde{D}^{-1}(\vec{s}_1 - \tilde{E}^T\vec{t}_2) = \tilde{D}^{-1}(\vec{s}_1 - \tilde{E}^T\vec{\hat{e}}). \tag{32}$$

Then we have to permute the solution vector $\vec{t}$ (see (28)) back to the vector $\vec{\tilde{e}}$ (see (20), (26)).

3. Using a preconditioner $\hat{M} = \hat{M}_1\hat{M}_2$ Equation (31) can be written as

$$\hat{M}_1^{-1}\hat{U}\hat{M}_2^{-1}(\hat{M}_2\vec{\hat{e}}) = \hat{M}_1^{-1}\vec{\hat{r}}. \tag{33}$$

Let be

$$\hat{M}_1 = \hat{D}_{\hat{U}}^{\frac{1}{2}}, \quad \hat{M}_2 = \hat{D}_{\hat{U}}^{\frac{1}{2}}, \quad \hat{D}_{\hat{U}} = diag(\hat{U}). \tag{34}$$

Combining (33) and (34) with (31) we obtain

$$\breve{U}\vec{\breve{e}} = \vec{\breve{r}}, \quad \breve{U} = \hat{D}_{\hat{U}}^{-\frac{1}{2}} \hat{U} \hat{D}_{\hat{U}}^{-\frac{1}{2}}, \;\; \vec{\breve{e}} = \hat{D}_{\hat{U}}^{\frac{1}{2}} \vec{\hat{e}}, \;\; \vec{\breve{r}} = \hat{D}_{\hat{U}}^{-\frac{1}{2}} \vec{\hat{r}}. \tag{35}$$

4. We construct an SSOR preconditioner for the matrix $\breve{U}$ (see (35)) [13] with a parameter ω. If the matrix $\breve{U}$ is decomposed as

$$\breve{U} = I + L + L^T \tag{36}$$

in its diagonal, strict lower, and strict upper triangular part, the SSOR matrices are defined as

$$\breve{M}_1 = (I + \omega L), \quad \breve{M}_2 = (I + \omega L^T) \quad \text{with} \quad 0 < \omega < 2. \tag{37}$$

We have to solve the system of linear algebraic equations

$$\breve{M}_1^{-1} \breve{U} \breve{M}_2^{-1} (\breve{M}_2 \vec{\breve{e}}) = \breve{M}_1^{-1} \vec{\breve{r}}. \tag{38}$$

We use Eisenstat's trick [14]. Because of (see (36))

$$\breve{M}_1^{-1} \breve{U} \breve{M}_2^{-1} = \frac{1}{\omega}((I + \omega L^T)^{-1} + (I + \omega L)^{-1}(I - (2 - \omega)(I + \omega L^T)^{-1}))$$

the matrix vector product $(\breve{M}_1^{-1} \breve{U} \breve{M}_2^{-1})v$, for any vector v, requires two solves [15] with the triangular matrices $(I + \omega L)$ and $(I + \omega L^T)$ plus a few arithmetical operations.

The Equations (38) are solved with Krylov subspace methods described in [16], [17], [18].

At present, we can handle structures with up to 3 million unknowns on modern workstations with a memory of half a GByte. The computing time for the solution of the linear algebraic equations are reduced compared to the original version [1], [3] by a factor of 10 (see section 7).

6 Eigenvalue Problem

The transverse electric mode fields $\vec{E}_{t,l}^{(p)}$ at the ports have to be computed before we can solve the system of linear equations. Because the transmission lines are longitudinally homogeneous any field can be expanded into a sum of so-called modal fields

$$\vec{E}(x, y, z \pm 2h) = \vec{E}(x, y, z)e^{\mp \jmath k_z 2h}, \tag{39}$$

which vary exponentially in the longitudinal direction. k_z is the propagation constant. $2h$ is the length of an elementary cell in z-direction. We consider the field components in three consecutive elementary cells. The electric field components of the vector $\vec{e}$ (see Equation (14)) $E_{x_{i,j,k+1}}$, $E_{x_{i,j,k-1}}$, $E_{y_{i,j,k+1}}$, $E_{y_{i,j,k-1}}$, $E_{z_{i,j,k-1}}$, $E_{z_{i+1,j,k-1}}$, and $E_{z_{i,j+1,k-1}}$ are expressed by the values of cell k using ansatz (39). The longitudinal electric field components E_z can be eliminated by means of the equation $BD_{A_{\tilde{\epsilon}}}\vec{e} = 0$ (see (13)) [7] . Thus, we get an eigenvalue problem for the transverse electric field on the transmission line region:

$$C\underline{\vec{e}} = \gamma\underline{\vec{e}} \ . \tag{40}$$

$\underline{\vec{e}}$ consists of components $E_{x_{i,j,k}}$ and $E_{y_{i,j,k}}$, $k = const$, of the eigenfunctions. Thus, the problem for the transmission line is reduced to a two dimensional problem. The sparse matrix C is non-symmetric or non-Hermitian in the lossless or the lossy case, respectively. The order of C is $2n_x n_y - n_b$. $n_x n_y$ is the number of elementary cells at the port. The size of n_b depends on the boundary conditions at the port. The relations between the eigenvalues γ and the propagation constants k_z are

$$\gamma = e^{-\jmath k_z 2h} + e^{+\jmath k_z 2h} - 2 = -4\sin^2(k_z h) = u + \jmath v, \tag{41}$$

$$k_z = \frac{\jmath}{2h}\ln\left(\frac{\gamma}{2} + 1 + \sqrt{\frac{\gamma}{2}\left(\frac{\gamma}{2} + 2\right)}\right) = \beta - \jmath\alpha. \tag{42}$$

A propagation constant k_z and its corresponding eigenfunction is called a mode. The energy of the complex and evanescent modes decreases exponentially with the distance from the discontinuity. Thus, in technical applications most of the modes can be neglected within the limit of accuracy. Generally speaking, the larger the magnitude of the imaginary part of k_z the

stronger the decay. Therefore, to sort the propagation constants according to their importance in our problem, we use the

Criterion: The propagation constants k_z are sorted in ascending order of $\mid \alpha \mid$. In the case that some $\mid \alpha \mid$ have the same value the constants k_z are sorted in descending order of $\mid \beta \mid$.

Computing the wanted propagation constants and the corresponding eigenfunctions the transverse electric fields $\vec{E}_{t,l}^{(p)}$, $l = 1(1)m^{(p)}$, are known at the ports p, and the boundary condition (6) can be built superposing the transmission line modes. In an earlier version of the method [3], [12] the complete set of eigenvalues and of corresponding propagation constants was computed and sorted in order to select the interesting propagation constants. The sparse matrix was stored as a dense matrix.

We avoid the computation of all eigenvalues to find the few required propagation constants using the implicitly restarted Arnoldi method [8], [9]. The sparse storage technique is applied.

The Arnoldi algorithm is called iteratively to solve the standard eigenvalue problem using the inverse mode $C^{-1}x = \frac{1}{\gamma}x$ with the solution of linear algebraic equations. In general the method does not converge using the regular mode for our eigenvalue problem. We use a combined unifrontal/multifrontal method [10] for the solution of large sparse sets of ill-conditioned unsymmetric linear equations.

By means of the Arnoldi iteration we can compute a set of eigenvalues of largest or smallest magnitude, real part or imaginary part, but we cannot find in one step the set of eigenvalues according to our criterion. Therefore, we must proceed in two steps.

In a first run we compute a subset $\mathcal{E}$ of eigenvalues γ of smallest magnitude using the Arnoldi method in inverse mode looking for eigenvalues of largest magnitude, and compute the corresponding subset $\bar{\mathcal{E}}$ of propagation constants. However, we have to find a subset $\bar{\mathcal{A}}$ of propagation constants with the smallest magnitude of the imaginary part, but possibly with large real part. In general, we have $\bar{\mathcal{A}} \cap \bar{\mathcal{E}} \neq \emptyset$ but $\bar{\mathcal{A}} \not\subseteq \bar{\mathcal{E}}$.

To search for the corresponding additional eigenvalues, we use a second run of the Arnoldi method with a modified matrix.

The wave number

$$k_f = \omega\sqrt{\epsilon\mu} = k_0\sqrt{\tilde{\epsilon}\tilde{\mu}} \tag{43}$$

is an upper bound for the interesting propagation constants of undamped modes in a waveguide. Using the maximum wave number $k^{(max)}$ of the cells

we extend the matrix C by a diagonal matrix which consists of the negative elements

$$\gamma_\tau^{(a)} = \gamma^{(max)}(1 + \frac{\tau}{10}), \;\; \tau = 1(1)m_a, \quad \gamma^{(max)} = -4(hk^{(max)})^2. \tag{44}$$

In a second run we compute a subset $\mathcal{E}^l$ of $m_a + m_r$ eigenvalues of smallest real part of the extended matrix C^* using the Arnoldi method in inverse mode. m_r is the number of negative eigenvalues of the subset $\mathcal{E}$ computed in the first run. Separating the m_n new eigenvalues of $\mathcal{E}^l$ and computing the corresponding propagation constants we have found all propagation constants according to our criterion if $m_n < m_a$. Otherwise we have to increase m_a for a new computation [11].

The modes satisfy the orthogonality relation (8) if $k_{z_l} \neq \mp k_{z_m}$. In the case of multiple eigenvalues the eigenfunctions are orthogonalized according to (8) using the method of Gram-Schmidt.

7 Numerical Results

The main steps of the Finite Difference Method in Frequency Domain

1. Generation of the two dimensional (port) and three dimensional (discontinuity) geometric structure and of the material dates,

2. Solution of the eigenmode problem,

3. Solution of the three dimensional boundary value problem (system of linear algebraic equations) and calculation of the scattering matrix

are implemented in apart programs. The time and memory consuming parts are the solution of the eigenmode problem and the solution of the system of linear algebraic equations. The number of eigenvalue problems to be solved depends on the number of ports (see Figure 1). The number of systems of linear algebraic equations to be solved depends on the number of ports and of modes. In general the steps (2.) and (3.) have to be done for several frequencies ω (see Eqn. (4)).

The reduction of the computing time is demonstrated calculating the scattering matrix of a structure consisting of coupled spiral inductors. The structure is assumed to be lossfree. The structure represented in Figure 1 is symmetric along the z-direction. Using appropriate boundary conditions it

will do to discretize the right-hand side of the structure only. The right-hand side of the structure is divided into $n_{xyz} = n_x n_y n_z = 239\,040$ elementary cells with $n_x = 30$, $n_y = 83$, and $n_z = 96$.

For the eigenmode problem the reduction of the computing time is demonstrated too by a second application using the algorithms in complex arithmetics (lossy case).

The time data in the Tables 1 and 2 refer to a SGI-Server Origin2000 with a memory of 4 GBytes. The execution times are given in seconds.

7.1 Numerical Example for the System of Linear Algebraic Equations

The order of the system of linear algebraic equations is $n = 3n_{xyz} = 717\,120$. The total number of nonzeros of the matrix $\tilde{U}$ (26) amounts to $4\,501\,636$ for this example where only $nnz = 2\,609\,378$ elements are stored. We apply an independent set ordering to the matrix $\tilde{U}$ (27) to obtain the reduced matrix $\hat{U}$(29). The order of the reduced system of linear equations (30) is $n_r = 323\,982$. The total number of nonzeros of the matrix $\hat{U}$ amounts to $5\,909\,142$. The number of stored nonzeros is $nnz_r = 3\,116\,562$.

The structure under investigation contains two ports. We take into account one mode at each port. Thus, we have to solve two systems of linear algebraic equations with the same coefficient matrix.

We now consider four possibilities of preconditioning for the given coefficient matrix $\tilde{U}$ to solve the linear system of equations (26).

1. The Eqn. (26) is to be solved with Jacobi-preconditioning.

$$\tilde{D}_{\tilde{U}}^{-\frac{1}{2}} \tilde{U} \tilde{D}_{\tilde{U}}^{-\frac{1}{2}} (\tilde{D}_{\tilde{U}}^{\frac{1}{2}} \tilde{e}) = \tilde{D}_{\tilde{U}}^{-\frac{1}{2}} \tilde{r} \quad , \quad \tilde{D}_{\tilde{U}} = diag(\tilde{U}).$$

2. The Eqn. (35) is to be solved.

$$\hat{D}_{\hat{U}}^{-\frac{1}{2}} \hat{U} \hat{D}_{\hat{U}}^{-\frac{1}{2}} (\hat{D}_{\hat{U}}^{\frac{1}{2}} \hat{e}) = \hat{D}_{\hat{U}}^{-\frac{1}{2}} \hat{r} \quad , \quad \hat{D}_{\hat{U}} = diag(\hat{U}).$$

3. The Eqn. (38) is to be solved with $\omega = 1,51$.

$$\breve{M}_1^{-1} \breve{U} \breve{M}_2^{-1} (\breve{M}_2 \vec{\breve{e}}) = \breve{M}_1^{-1} \vec{\breve{r}} \quad , \quad \breve{M}_2^T = \breve{M}_1 = (I + \omega L).$$

4. The Eqn. (38) is to be solved with the parameter $\omega = 1,51$ by using Eisenstat's trick [14].

	Original version	Version 1	Version 2	Version 3	Version 4
Iterations	5333	5374	3150	935	935
Iteration time [s]	6541	3316	1406	914	633
Total time [s]	6549	3329	1429	936	657

Table 1: Performance comparisions of different preconditioners compared to the original version for the calculation of the scattering matrix of the right-hand side of the structure consisting of coupled spiral inductors.

We compare the performance of the four different preconditioners with the original version described in [1] and [3]. The number of iterations and executions times are given in Table 1. The systems of algebraic equations were solved by the algorithm described in [17]. The stopping criterion was in each case a reduction of the norm of the residual by 10^{-8} for the four kinds of preconditioning and the original version, respectively. Both the time for the iteration algorithm and the total time for the subroutine call are given. The SSOR preconditioner combined with the independent set ordering is very effective in solving the linear systems of equations. Furthermore, Eisenstat's trick reduces the time for the iteration algorithm.

7.2 Numerical Examples for the Eigenvalue Problem

The computation of all eigenvalues with the QR algorithm and the calculation of the eigenfunctions of the wanted propagation constants by solving systems of linear homogeneous algebraic equations in the original version [1], [3], [12] is very time and memory consuming. Computing the wanted propagation constants only, using of the sparse storage technique, and neglecting relatively small elements in the matrix C (see (40)) reduce the computing time considerably.

Detailed comparisions between the original and the new version are presented for two applications in Table 2.

The first example refers to the coupled spiral inductors (see Figure 1 and section 7.1). The eigenvalue problem is solved for one port. We take into account three modes at the port. The sparse matrix C of the eigenvalue problem (see (40)) is non-symmetric.

The second application concerns a different structure with lossy material.

The corresponding matrix of (40) is non-Hermitian. The number of modes which have to be computed is four.

The dimensions of the eigenvalue problems are given in the second column of Table 2. The maximum number of nonzeros in a row of C is 9. The total number nze of nonzero elements of the matrix C is given in the third column of Table 2. The time measurements involve matrix generation, solving the eigenvalue problem and computation the mode fields.

	Dimension	nze	Original version [s]	New version [s]
lossfree case	4366	21136	9491	2
lossy case	5286	29906	79040	331

Table 2: Comparisions of computing times for the eigenvalue problem between the original and the new version for a lossfree and a lossy example.

Taking into account that an eigenmode problem generally is to be solved for some angular frequencies ω (see section 3) and for more than one port the computing time is reduced from days to minutes for a non-Hermitian matrix C of order $2n_xn_y - n_b = 5286$ (see (40)). The total storage requirement is reduced by a factor 18 in the new version for this example.

References

[1] Beilenhoff, K., Heinrich, W., Hartnagel, H. L.: Improved Finite-Difference Formulation in Frequency Domain for Three-Dimensional Scattering Problems, IEEE Transactions on Microwave Theory and Techniques, Vol. 40, No. 3, 540-546 (1992)

[2] Christ, A., Hartnagel, H. L.: Three-Dimensional Finite-Difference Method for the Analysis of Microwave-Device Embedding, IEEE Transactions on Microwave Theory and Techniques, Vol. MTT-35, No. 8, 688-696 (1987)

[3] Christ, A.: Streumatrixberechnung mit dreidimensionalen Finite-Differenzen für Mikrowellen-Chip-Verbindungen und deren CAD-Modelle, Fortschrittberichte VDI, Reihe 21: Elektrotechnik, Nr. 31, 1-154 (1988)

[4] Hebermehl, G., Schlundt, R., Zscheile, H., Heinrich, W.: Improved Numerical Solutions for the Simulation of Monolithic Microwave Integrated Circuits, Preprint No. 236, Weierstraß-Institut für Angewandte Analysis und Stochastik im Forschungsverbund Berlin e.V., 1-43 (1996)

[5] Yee, K. S.: Numerical Solution of Initial Boundary Value Problems Involving Maxwell's Equations in Isotropic Media, IEEE Transactions on Antennas and Propagation, Vol. AP-14, No. 3, 302-307 (1966)

[6] Weiland, T.: Eine numerische Methode zur Lösung des Eigenwellenproblems längshomogener Wellenleiter, Archiv für Elektronik und Übertragungstechnik, Band 31, Heft 7/8, 308-314 (1977)

[7] Hebermehl, G., Schlundt, R., Zscheile, H., Heinrich, W.: Simulation of Monolithic Microwave Integrated Circuits, Preprint No. 235, Weierstraß-Institut für Angewandte Analysis und Stochastik im Forschungsverbund Berlin e.V., 1-37, (1996)

[8] Sorensen, D. C.: Implicit Application of Polynomial Filters in a k-Step Arnoldi Method, SIAM J. Matr. Anal. Apps., 13, 357-385 (1992)

[9] Lehoucq, R. B.: Analysis and Implementation of an Implicitly Restarted Arnoldi Iteration, Rice University, Technical Report TR95-13, Department of Computational and Applied Mathematics, 1-135 (1995)

[10] Davis, T. A., Duff, I. S.: A combined Unifrontal/Multifrontal Method for Unsymmetric Sparse Matrices, University of Florida, Technical Report TR97-016, 1-18 (1997)

[11] Hebermehl, G., Schlundt, R., Zscheile, H., Heinrich, W.: Eigen Mode Solver for Microwave Transmission Lines, The International Journal for Computation and Mathematics in Electrical and Electronic Engineering, Vol. 16, No. 2, 108-122 (1997)

[12] Klingbeil, H., Beilenhoff, K., Hartnagel, H. L.: FDFD Full-Wave Analysis and Modeling of Dielectric and Metallic Losses of CPW Short Circuits, IEEE Transactions on Microwave Theory and Techniques, Vol. 44, No. 3, 485-487 (1996)

[13] Barret, R., Berry, M., Chan, T., Demmel, J., Donato, J., Dongarra, J., Eijkhout, V., Pozo, R., Romine, C., van der Vorst, H.: Templates for

the Solution of Linear Systems: Building Blocks for Iterative Methods, SIAM, Philadelphia, PA, (1994)

[14] Eisenstat, S. C.: Efficient Implementation of a Class of Preconditioned Conjugate Gradient Methods, SIAM J. Sci. Statist. Comput. 2, 1-4, (1981)

[15] Hebermehl, G., Schlundt, R., Zscheile, H., Heinrich, W.: Improved Numerical Solutions for the Simulation of Microwave circuits, Preprint No. 309, Weierstraß-Institut für Angewandte Analysis und Stochastik im Forschungsverbund Berlin e.V., 1-15, (1997)

[16] Paige, C.C., Saunders, M.A.: Solution of Sparse Indefinite Systems of Linear Equations, SIAM J. Numer. Anal. 12, 4, 617-629 (1975)

[17] Freund, R.W., Nachtigal, N.M.: A new Krylov-subspace method for symmetric indefinite linear systems, AT&T Numerical Analysis Manuscript, Bell Labs, Murry Hill, NJ, 1-8 (1994)

[18] Deuflhard, P.: A Study of Lanczos-Type Iterations for Symmetric Indefinite Linear Systems, Preprint SC 93-6, Konrad-Zuse-Zentrum für Informationstechnik Berlin, 1-19, (1993)